THE JOURNAL OF BIOLOGICAL CHEMISTRY
Vol. 270, No. 13, Issue of March 31, pp. 7523–7532, 1995
Printed in U.S.A.

Characterization of Sialyloligosaccharide Binding by Recombinant Soluble and Native Cell-associated CD22

EVIDENCE FOR A MINIMAL STRUCTURAL RECOGNITION MOTIF AND THE POTENTIAL IMPORTANCE OF MULTISITE BINDING*

(Received for publication, November 30, 1994, and in revised form, January 13, 1995)

Leland D. Powell‡§, Rakesh K. Jain¶, Khushi L. Matta¶, Subramaniam Sabesan‖, and Ajit Varki‡

From the ‡Glycobiology Program and UCSD Cancer Center, Department of Medicine, University of California at San Diego, La Jolla, California 92093, ¶Gynecologic Oncology Research, Roswell Park Cancer Institute, Buffalo, New York 14263, and ‖Central Science & Engineering, DuPont Co., Wilmington, Delaware 19880

CD22, a B cell-specific receptor of the immunoglobulin superfamily, has been demonstrated to bind to oligosaccharides containing α2–6-linked sialic acid (Sia) residues. Previously, we demonstrated that the minimal structure recognized by this lectin is the trisaccharide Siaα2–6Galβ1–4GlcNAc, as found on *N*-linked, *O*-linked, or glycolipid structures (Powell, L., and Varki, A. (1994) *J. Biol. Chem.* 269, 10628–10636). Here we utilize a soluble immunoglobulin fusion construct (CD22Rg) to determine directly by equilibrium dialysis the stoichiometry (2:1) and dissociation constant (32 μM) for Neu5Acα2–6Galβ1–4Glc binding. Inhibition assays performed with over 30 different natural and synthetic sialylated and/or sulfated compounds are utilized to define in greater detail specific structural features involved in oligosaccharide-protein binding. Specifically, the critical features required for binding include the exocyclic hydroxylated side chain of the Sia residue and the α2–6 linkage position to the underlying Gal unit. Surprisingly, alterations of the 2-, 3-, and 4-positions of the latter residue have limited effect on the binding. The nature of the residue to which the Gal is attached may affect binding. Bi(α2–6)-sialylated biantennary oligosaccharides are capable of simultaneously interacting with both lectin sites present on the dimeric CD22Rg fusion construct, giving a marked improvement in binding over monosialylated compounds. Furthermore, data are presented indicating that full-length native CD22, expressed on the surface of Chinese hamster ovary cells, is structurally and functionally a multimeric protein, demonstrating a higher apparent affinity for multiply sialylated compounds over monosialylated compounds. These observations provide a mechanism for strong CD22-dependent cell adhesion despite the relatively low K_d for protein-sugar binding.

CD22 is a sialic acid (Sia)[1] binding glycoprotein found predominantly on resting IgM^+IgD^+ B cells (1–5). It binds to oligosaccharides containing the sequence Siaα2–6Galβ1–4Glc/GlcNAc, and shows no affinity for oligosaccharides containing α2–3-linked Sia residues. By sequence analysis, it is a member of the immunoglobulin superfamily, with an N-terminal V-type domain followed by six Ig C2-type domains, a membrane spanning region, and a 160-amino acid cytoplasmic tail (6–9). Two isoforms of human CD22 have been identified by cDNA cloning, a seven domain CD22β form and a shorter CD22α form, which lacks the third and fourth domains present in CD22β. The extent of tissue expression of these two isoforms is at present unexplored, although most cells examined appear to express the larger isoform (10). Murine CD22β shows a 62% sequence homology to the human form and, likewise, a lectin activity directed toward α2–6-linked sialyloligosaccharides (9, 11).

In vitro assays have demonstrated that CD22β (hereafter referred to as CD22) functions in a dual capacity, both as an adhesion molecule and as an activation molecule. Cells induced to express CD22 by cDNA transfection acquire the ability to adhere to a variety of different cell types, including erythrocytes, lymphocytes (both T and B cells), and a variety of transformed cell lines (7–9, 12, 13). In certain cases, a higher level of binding has been demonstrated with cell activation, which seems to correlate with increased expression of β-galactoside α2,6-sialyltransferase (8, 9), the enzyme that synthesizes the Siaα2–6Galβ1–4GlcNAc sequence (14, 15). A role in activation is indicated by the observations that CD22 defines the subset of IgM^+ B cells which show increased levels of intracellular Ca^{2+} in response to stimulation with anti-μ, and that anti-CD22 augments this response (16). Moreover, anti-μ stimulation of B cells rapidly induces the phosphorylation of cytoplasmic Tyr residue(s) on CD22, and a small percentage of surface CD22 (≤2%) may be found in association with the B cell-sIg complex, including both IgM or IgG of naive or memory B cells (17–19). In addition to playing a role with B cell activation, CD22 participates in T cell activation. CD22 binds to several T cell glycoproteins, including CD45, and binding of soluble CD22 to CD45 attenuates the increase in intracellular calcium normally seen in T cells following stimulation with anti-CD3 (8, 12).

In a series of experiments utilizing both the full-length CD22β molecule expressed in COS cells or a truncated three domain construct fused to the Fc portion of Ig (CD22Rg), we and others have demonstrated that its ability to bind to cells or

* This work was supported by National Institutes of Health Grants GM32373 (to A. V.) AI29326 (to K. L. M.) and Clinical Investigator Award KO1 CA01649 (to L. D. P.) and by American Cancer Society Institutional Grant ACS-IRG93W (to L. D. P.). The costs of publication of this article were defrayed in part by the payment of page charges. This article must therefore be hereby marked "*advertisement*" in accordance with 18 U.S.C. Section 1734 solely to indicate this fact.

§ To whom correspondence should be addressed: Cancer Center 0063, UCSD School of Medicine, La Jolla, CA 92093-0063. Tel.: 619-534-2507; Fax: 619-534-5792.

[1] The abbreviations used are: Sia, sialic acid type unspecified; AGP, $α_1$-acid glycoprotein; CD22Rg, CD22-immunoglobulin chimera containing Ig domains 1–3 of human CD22β; DTSSP, 3,3′-dithiobis(sulfosuccinimidyl propionate); PNGase F, peptide *N*-glycosidase F; sLac, sialyllactose; SNA, *Sambucus nigra* agglutinin; IC_{50}, concentration giving 50% inhibition of binding; FGP, fibrinogen glycopeptides; RIC, relative inhibitory concentrations (IC_{50} relative to α2–6-sLac); PAGE, polyacrylamide gel electrophoresis; CHO, Chinese hamster ovary; PBS, phosphate-buffered saline; ELISA, enzyme-linked immunosorbent assay; ONP, *o*-nitrophenyl.

precipitate glycoproteins from cell lysates is dependent on the presence of Sia residues on the target cells or molecules (8, 20, 21). A sensitive column assay showed that CD22 has a low but detectable affinity for sialylated *N*-linked oligosaccharides, providing that the Sia residues are α2–6-linked. In contrast, α2–3-linked residues are not bound. Using purified β-galactoside α2,6-sialyltransferase to sialylate a variety of complex oligosaccharide structures, we further demonstrated that CD22Rg recognizes only the trisaccharide Siaα2–6Galβ1–4Glc/NAc. Other structural features in complex *N*-linked oligosaccharides, including branching, fucosylation, and/or other core region sugars, were not recognized. However, a higher apparent affinity was observed for multisialylated structures, implying that the CD22Rg construct was capable of interacting with adjacent α2–6-Sia residues present on the same molecule. However, this column assay could not exclude higher apparent binding merely due to a higher density of α2–6-Sia residues on a single oligosaccharide.

To further understand the lectin properties of this molecule, several assay systems including equilibrium dialysis, ELISA capture, column binding, and cell adhesion, are utilized here to examine the binding of CD22Rg to a number of different mono- and bisialylated compounds. Additionally, cross-linking experiments have been performed to explore the possibility that cell-surface CD22 might be present in a multimeric form. These experiments, together with additional work in the accompanying papers (22, 23) examining the role of CD22 in cell-adhesion events, offer new insights into how this Sia-specific lectin may function in complex biological systems.

EXPERIMENTAL PROCEDURES

Equilibrium Dialysis—Equilibrium dialysis was performed in a microdialyzer chamber consisting of 3/16 inch diameter holes in leucite, manufactured locally, utilizing CE M_r cut-off 100,000 membranes (25 μm thick; No. 132966, Spectrum Medical Industries, Houston, TX). Use of thicker membranes, even of M_r cut-off 50,000, gave incomplete dialysis of some oligosaccharide ligands over 24 h. Samples were prepared utilizing the CD22β chimera (CD22Rg) constructed from the first three domains of CD22β fused to murine Ig (8), expressed by stable transfection in CHO cells (21), which do not synthesize α2–6-linked Sia residues (24, 25). The CD22Rg chimera purified from CHO cells was >90% pure (by SDS-PAGE utilizing Coomassie Blue staining). Protein concentration was determined by the BCA assay (Pierce), utilizing either bovine serum albumin (2 mg/ml stock solution, Pierce) or purified pooled human IgG (No. 14506, Sigma) as a standard. Pooled IgG was chosen as a standard, since CD22Rg is 40% IgG by construction with the remaining 60% (CD22) being a member of the immunoglobulin superfamily. Thus, CD22Rg might be expected to have a similar reactivity in this colorimetric assay. Both standards were within 95% agreement and thus the value obtained utilizing IgG as a standard was utilized to determine the concentration of CD22Rg solutions. As an additional confirmation of the validity of this determination, CD22Rg concentration was determined by A_{280}, utilizing the value of $A_{280}^{0.1\%} = 1.35$ for pooled human IgG. By this approach, the concentration of CD22Rg was determined to be only 15% higher than that determined by the BCA assay. Since the above A_{280} value for pooled IgG depends upon an average extinction coefficient which is not accurate for a single protein, the BCA values were used throughout. Samples containing CD22Rg (1–1.2 mg/ml, 5–5.1 μM protein, based on M_r = 210,000), 2–10 pmol of [^{3}H]α2–6-sLac, and 1–20 μmol of α2–6-sLac (final concentration 0.2–400 μM), in 50 μl of TBS (20 mM Tris-Cl, pH 7.4, 0.14 M NaCl, 0.02% azide) were dialyzed against 50 μl of TBS for 14–18 h at 4 °C. Experiments done in the absence of CD22Rg demonstrated complete equilibration of the [^{3}H]cα2–6sLac across the membrane over this time period. Thereafter, 25-μl aliquots were removed from each side of the membrane and counted by liquid scintillation spectrometry. From these data, the total, bound, and free concentrations of α2–6-sLac were calculated and the data analyzed according to Scatchard (26). Slope and intercepts were calculated by a linear least squares fit program provided by Cricket Graph (Cricket Software, Malvern, PA). Inclusion of 1 mM α2–6-sLac resulted in total competition of binding of the [^{3}H]α2–6-sLac in this assay.

Preparation of FGP—Bovine fibrinogen (Sigma) was utilized as a source of biantennary oligosaccharides containing one or two α2–6-linked sialic acid residues. Ten grams were dispersed in 250 ml of 0.1 M Tris-Cl, pH 8.0, 1.0 mM $MgCl_2$, 1 mM $CaCl_2$, 0.02% azide, and digested for 24 h at 50 °C with 500 mg of predigested Pronase (Calbiochem, San Diego, CA). At 24 h, fresh Pronase was added and the digestion continued for another 24 h. After partial concentration by lyophilization, the sample was desalted on Bio-Gel P-2 (Bio-Rad) in 4% pyridine, 2% acetic acid in water, and the V_0 (detected by the resorcinol assay) lyophilized. This material was digested once again with 50 mg of Pronase for 24 h. Thereafter, the pH was adjusted to 11.5 with concentrated NH_4OH and incubated at 37 °C for 3–4 h to remove any *O*-acetylation of Sia residues (known to interfere with binding to CD22Rg, see Ref. 13). The sample was neutralized with acetic acid, lyophilized, and desalted as above on Bio-Gel P-2. To remove the brown residue arising from the Pronase, the material was passed over a 10-ml column of lipophilic Sephadex (LH-60, Sigma) in pyridine/acetate buffer and then finally through a C_{18} SPICE cartridge (Analtech Inc., Newark, NJ), to yield a colorless material. The FGP prepared contained a mixture of mono- and bisialylated oligosaccharide chains, as determined by the amount of β-galactosidase releasable galactose before and after digestion with *Arthrobacter ureafaciens* sialidase (Calbiochem). A sample containing 10–20 nmol of Sia was digested with 20 milliunits of jack bean β-galactosidase (Oxford GlycoSystems, Rosedale, NY) with or without 10 milliunits of *A. ureafaciens* sialidase. Liberated Gal was detected by the Mopper-Gindler assay (27), which detects free reducing terminals of all hexoses. Sialic acid, a keto sugar, has a color yield only 17% that of Gal, on a molar basis, permitting the accurate detection of liberated Gal in the presence of the liberated NeuAc. By this approach, the FGP contained approximately 40% bisialylated structures, with the remainder being monosialylated structures. This preparation was utilized as the unlabeled FGP in Figs. 2 and 7. To prepare a population enriched in bisialylated structures, ~200 nmol were *N*-acetylated with acetic anhydride (28) to cap the free amino groups on the amino acid(s) and fractionated by high performance liquid chromatography on a Rainin SAX column, equilibrated with water, and developed with a gradient of 0.3 M NaCl, 20 mM Tris-Cl, pH 7.0. Two major and two minor resorcinol-positive peaks were detected, and by the approach described above, the second major peak identified to contain approximately 75% bisialylated structures. This enriched bisialylated material was used as an inhibitor for the ELISA assay described in Fig. 4.

Preparation of [^{3}H]FGP—Radiolabeled bi(α2–6)-sialylated FGP was prepared by treating a portion of the initial FGP preparation (~20 nmol) with UDP-Gal and bovine galactosyltransferase (Sigma), and then with CMP-[^{3}H]NeuAc and β-galactosyl α2,6-sialyltransferase (21). This material, when analyzed by binding to the CD22Rg protein A-Sepharose column (21), contained about 60% bisialylated structures and 40% monosialylated material. This material was preparatively separated into mono- and bisialylated structures on the CD22Rg column, to yield a radioactive bisialylated FGP glycopeptide whose elution corresponded to the pool III material described previously (21).

Synthetic Sialosides—The syntheses of the sialylated oligosaccharides **2–4**, **6–11**, and **26–29** (Table I) have been described elsewhere (29–31). Included are two diisopropylidene derivatives (**2** and **11**) which contain a Gal residue with two isopropylidene groups, alkylating the O_1-O_2 and the O_3-O_4 molecules. The synthesis of the sialylated, fucosylated, and/or sulfated oligosaccharides **12-25** (Table I) has been described elsewhere (32–35).

Sialic Acid Determinations—Sialic acid was quantitated by the acetylacetone assay (36), which quantitates the formaldehyde released after treatment with 1.25 mM $NaIO_4$. This assay is equally sensitive for both free and glycosidically bound sialic acids, unlike either the resorcinol or thiobarbituric acid assays. The same stock tube of Neu5Ac was used as a standard throughout.

Oligosaccharide-CD22Rg Binding Column Assay—A 2.5-mm diameter column, containing 0.15 ml of protein A-Sepharose containing 25–50 μg of CD22Rg, equilibrated in TBS (20 mM Tris-Cl, pH 7.4, 140 mM NaCl, 0.02% sodium azide), was prepared. A 30-μl sample containing 950 cpm of ^{3}H-bisialylated FGP (less than 0.1 nmol) was combined with 200 cpm of [^{14}C]Glc and either buffer alone or variable concentrations of other sialosides, as indicated in figure legends, and the column eluted at 4 °C collecting 0.12-ml fractions. On a column of this small size, quantitative recovery of the ^{3}H-labeled bisialylated FGP is achieved at 4 °C, and warming to ambient temperature as performed previously was not required (21).

ELISA Assays—An ELISA capture assay was developed to screen the ability of different sialylated oligosaccharides to inhibit the binding of CD22Rg to a sialoglycoprotein. Working at 4 °C, 200 ng of pooled human IgM (Calbiochem) or 1–2 μg of human α_1-acid glycoprotein (AGP, Sigma) were bound to microtiter wells (Immulon 4, Fisher Sci-

entific Co., Tustin, CA) in PBS (for IgM) or 50 mM Tris-Cl, pH 10 (for AGP), for 18–36 h. After blocking with PBS, 1% bovine serum albumin (3–4 h), 2–3 μg of CD22Rg in 100 μl of TBS, with or without the indicated sugar inhibitor, were added and incubated for 18 h. The plates were rinsed twice with TBS, incubated for 2 h with 100 μl/well of horseradish peroxidase-conjugated goat anti-murine IgG sera (Bio-Rad; 1/200 dilution in TBS, 0.1% Nonidet P-40), and then rinsed 4 times, 5 min/rinse, with TBS/Nonidet P-40. The wells were developed with *o*-phenylenediamine, and A_{560} read with a MicroTek plate reader. Assays were performed in duplicate throughout. For each set of experiments, α2–6-sLac was included as a positive reference compound. As the IC_{50} for α2–6s-Lac ranged from 30 to 120 μM between assays, the relative inhibitory concentration (RIC) of a given compound was calculated as the ratio of IC_{50} values for a test compound to α2–6-sLac.

Creation of CD22-CHO Cells—Stably transfected cell lines were established as described (21), utilizing a plasmid coding for the full-length transmembrane form of CD22β (8). Colonies (lifted by EDTA) were screened for CD22 expression using phycoerythrin-conjugated Leu-14 monoclonal antibody (Becton Dickinson, Oxnard, CA); and flow cytometry utilizing a FACscan® instrument (Becton Dickinson Immunocytometry Systems, Mountain View, CA).

Plate Adherence Assay—Daudi cells, a human B cell lymphoma line, were labeled for 18 h with [^{3}H]thymidine (DuPont NEN, Wilmington, DE), washed 3 times in PBS, 0.5% bovine serum albumin, and adjusted to 5 × 10^5/ml in PBS, 0.5% bovine serum albumin, 2 mM $MgCl_2$. Confluent wells of a 48-well tray containing either CHO or CD22-CHO cells were rinsed 3 times with PBS. Samples (100 μl) containing α2–6s-Lac, FGP, or no inhibitor, were added, incubated at 4 °C on an orbital shaker (100 rpm) for 30 min, and rinsed four times with ice-cold TBS. Bound cells were lifted with 0.4 ml of TBS/Nonidet P-40 and quantitated by liquid scintillation counting. Each inhibitor concentration was studied in triplicate.

Cross-linking Studies—CD22-CHO cells were metabolically labeled with [^{35}S]EXPRE^{35}S^{35}S (DuPont NEN) for 12 h in methionine-free media, then chased with complete media for 4 h. Working at 4 °C, cells were lifted with PBS, 2 mM EDTA, washed in PBS, and then cross-linked with 0–3 mM DTSSP (Pierce). After quenching excess cross-linker with 10 mM Tris-Cl in PBS, cells were lysed (21) in the presence of aprotinin and phenylmethylsulfonyl fluoride, lysates were preadsorbed with protein A-Sepharose (3 h) and then adsorbed with anti-CD22 (To15, Dako Corp., Carpenteria, CA) and protein A-Sepharose for 12 h. Antigen-resin complexes were washed sequentially with TBS, Nonidet P-40, 2 mM EDTA; TBS, Nonidet P-40, 2 mM EDTA, 1.0 M NaCl; TBS, 1% Nonidet P-40, 0.1% SDS, 0.1% cholate; and finally with 50 mM Tris-Cl, 0.1% Nonidet P-40. Bound proteins were eluted with SDS-PAGE sample buffer lacking reducing agents, and one-half of each sample was reduced (1% dithiothreitol). Reduced and nonreduced samples were boiled for 2 min and analyzed by SDS-PAGE (6%), followed by fluorography.

Similarly prepared radioactive lysates were subjected to immunoprecipitation with CD22Rg in the absence or presence of α2–6-sLac, utilizing the same washing procedure. Total amount of precipitable radioactivity was determined, and the samples analyzed by SDS-PAGE/fluorography.

RESULTS

Equilibrium Dialysis Analysis of CD22-α2–6-sLac Binding—Previous work established that CD22 functions as a sialic acid-specific lectin (8, 21, 37). These studies were performed both with the native transmembrane CD22β molecule, transiently expressed in COS cells, as well as with a fusion protein termed CD22Rg. The latter was formed by the fusion of the first three N-terminal domains of CD22β with the hinge and two C-terminal domains of human IgG_1 (8), forming a protein with an apparent M_r of 210,000 and 105,000 under nonreducing and reducing conditions by SDS-PAGE, respectively (data not shown). Thus, the native molecule is a dimer, akin to native immunoglobulins, and some of its binding properties may be due to the proximity of two identical lectin sites, located in the first three domains. To further examine the sialic acid-lectin properties of CD22, we directly examined the binding of the chimera to [^{3}H]α2–6-sLac by equilibrium dialysis, performed at 4 °C. These results (see Fig. 1, which includes data pooled from three experiments) demonstrate the presence of two binding sites (n = 2.2) per dimeric 210,000 M_r chimera, consistent with the presence of a single sialic acid-binding site located in one of the first three N-terminal domains of CD22β. This stoichiometry is based on protein concentration determined by the BCA protein assay, using human IgG as a standard. Determination of protein concentration by A_{280} was in close agreement (see "Experimental Procedures"). The apparent binding affinity for α2–6-sLac is 32 μM.

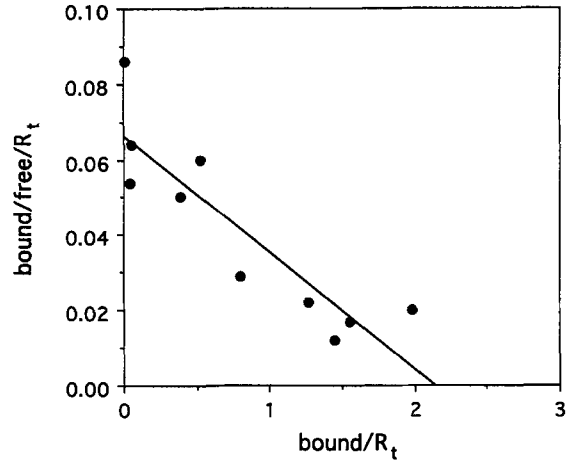

FIG. 1. **Equilibrium dialysis binding of α2–6-sLac to CD22Rg.** CD22Rg (5 μM protein concentration based on a M_r of 210,000) was incubated with increasing amounts of unlabeled α2–6-sLac in the presence of a fixed amount (2–4 pmol) of [^{3}H]2–6-sLac, in a total volume of 50 μl. Dialysis was against 50 μl of buffer, across a M_r cut-off 100,000 dialysis membrane, for 18 h at 4 °C. Aliquots were taken from either side of the membrane and counted, the concentration of bound and free α2–6-sLac determined, and the data plotted according to Scatchard. The data were fit to a single line by a linear least squares program. The slope corresponds to a K_d of 32 μM, and the x intercept indicates a stoichiometry of 2.2. R_t, total concentration of receptor in (μM).

Previously, we utilized a column elution assay to determine CD22Rg-oligosaccharide binding (21, 37). By this approach, sialylated oligosaccharides with two or more α2–6-linked Sia residues were found to be retained longer as compared to monosialylated structures. This observation suggested tighter binding of bisialylated structures with the two possible binding sites on the dimeric CD22Rg chimera. To more quantitatively study interactions with a bisialylated biantennary oligosaccharide, Pronase glycopeptides were generated from bovine fibrinogen, which contains exclusively biantennary *N*-linked structures containing only α2–6-linked Sia residues (38). On several batches of commercial fibrinogen examined, sialylation was incomplete, and large quantities of pure bisialylated material could not be generated. However, as described under "Experimental Procedures," a small quantity of radioactive bisialylated material could be generated using glycosyltransferases and ion exchange chromatography. This material was employed in a "single point" dialysis experiment utilizing radiotracer amounts of either [^{3}H]α2–6-sLac or ^{3}H-bisialylated FGP. Under conditions of large excess of lectin over ligand, the free receptor concentration closely approximates the total receptor concentration (R_t). Thus, provided the stoichiometry is known or can be estimated, the K_d can be calculated directly from the ratio of bound to free ligand and the R_t. By this approach, a bisialylated glycopeptide, prepared from fibrinogen, exhibited a 17-fold higher apparent affinity to CD22Rg than α2–6-sLac. This ratio would correspond to an apparent K_d of 1–2 μM.

The enhanced binding affinity of the bisialylated FGP over that of α2–6-sLac was further demonstrated by examining their ability to inhibit the binding of a radiolabeled oligosaccharide to immobilized CD22Rg. The CD22Rg columns initially

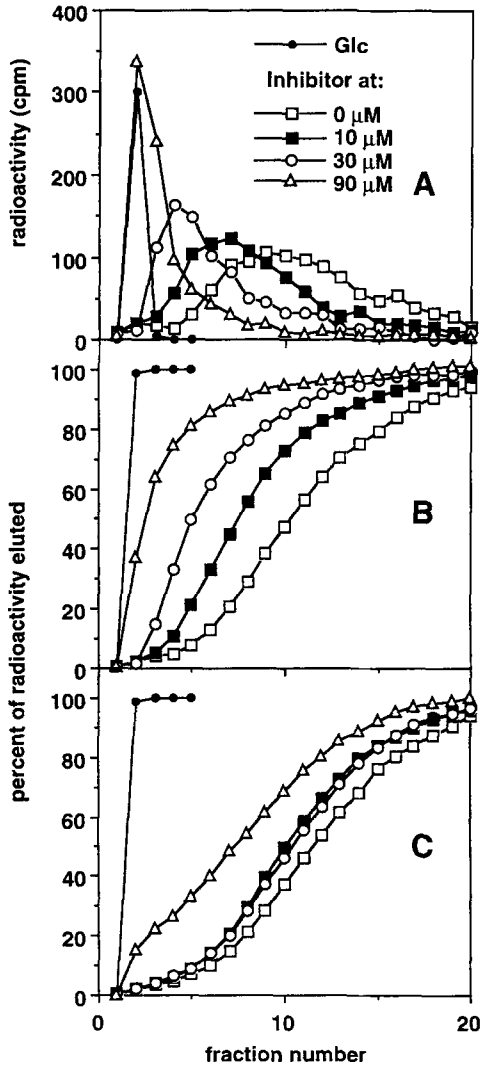

FIG. 2. **Comparison of α2-6-sLac and FGP as inhibitors of [^{3}H]FGP binding to CD22Rg.** A 30-μl sample containing bisialylated [^{3}H]FGP (less than 0.1 nmol), combined with [^{14}C]Glc and buffer alone (□), 10 μM (■), 30 μM (○), or 90 μM (△) of unlabeled FGP (a mixture of mono and bisialylated structures), was applied to CD22Rg-PAS and eluted at 4 °C (*Panel A*). The elution profile of [^{14}C]Glc for only one of the four runs is also shown (●). From these data, a running sum on a percentage basis of the eluted radioactivity was calculated, and is presented in *Panel B*. A similar series of experiments was done with 0, 10, 30, and 90 μM α2–6-sLac, and these data are presented only as a running sum in *Panel C* (*symbols* as in *Panel A*).

utilized to demonstrate oligosaccharide binding contained ≥200 μg of protein, and the elution of most multisialylated compounds required warming the column to 22–24 °C (21, 37). A new column was constructed which contained ~25–50 μg of protein on 0.15 ml of protein A-Sepharose. With a column of this small scale, the [^{3}H]FGP, applied in a total volume of 30 μl, eluted significantly slower than the nonbinding [^{14}C]Glc marker (Fig. 2), and warming of the column was not required for successful elution. When this same 30-μl sample, containing 10–90 μM unlabeled FGP (with concentrations based on Sia groups, not peptide), is applied to the column, the radioactivity elutes significantly earlier (Fig. 2*A*). These column profiles can be presented with greater clarity by calculating a running sum, on a percentage basis, of the eluted radioactivity (Fig. 2*B*). In contrast to this result, when 10–90 μM α2–6-sLac is included, significantly less inhibition of the binding of the [^{3}H]FGP is observed (Fig. 2*C*). As a greater level of inhibition is seen with FGP than α2–6-sLac for identical concentrations of competing α2–6-Sia groups, then the FGP must have an intrinsically higher affinity for CD22Rg than with α2–6-sLac. These results are consistent with those of the single point dialysis experiment. The most likely mechanism for this increased affinity would be its ability to simultaneously interact with more than one sialic acid binding site. Alternatively, other segments of the *N*-linked glycopeptides may interact with CD22Rg (*e.g.* Man residues, chitobiose core sugars). However, in prior investigations we have found no evidence to suggest that other structural features on an *N*-linked oligosaccharide are recognized by CD22Rg (37).

Sialyloligosaccharide Binding Specificity of CD22—To further define structural features recognized by CD22, a number of chemically synthesized glycosides were screened as inhibitors in an ELISA assay using either IgM or AGP coated onto microtiter wells. While the accompanying papers (22, 23) show that interactions of these proteins with CD22 is strictly Sia-dependent, IgM was found to be a more reliable reagent for these assays as (*a*) IgM intrinsically has a much higher apparent affinity for CD22Rg (23); (*b*) a good signal with IgM required only 100–200 ng/well, as compared with 1 μg/well of AGP; (*c*) significant lot-to-lot variability in AGP was found (which paralleled total Sia content); and (*d*) immunoglobulins adhere to polystyrene surfaces more efficiently than highly glycosylated proteins such as AGP. Wells coated with IgM were incubated with 20 μg/ml CD22Rg in the absence or presence of a potential inhibitor at various concentrations, and the bound chimera detected with horseradish peroxidase-conjugated goat anti-mouse immunoglobulin antisera. The structures of the compounds examined, and the numbering scheme employed in Figs. 3–5, are listed in Table I. By this assay, the IC_{50} of α2–6-sLac ranged between 30 and 120 μM (*e.g.* Fig. 3, *A* and *D*), a result consistent with its K_d determined from equilibrium dialysis (Fig. 1). The variability most likely reflects intrinsic limitations of the assay and differences in reagents employed, as these experiments were conducted over 6 months time. In each series of experiments, α2–6-sLac was included as a reference compound, and the RIC of these different compounds to α2–6-sLac are summarized in Table I.

These experiments indicate that CD22Rg is capable of binding a broad range of α2–6-sialosides and, moreover, that structural features away from the Sia residue may significantly influence CD22Rg binding. In confirmation of prior studies, α2–3-linked Sia residues are not recognized (**5**, Fig. 3). Several molecules containing a 6-thio derivative of Gal (**2**, **3**, **7**, **8**, **9**, and **11**) were examined. These compounds were originally developed as (potentially) nonhydrolyzable inhibitors for different bacterial and viral sialidases (31). All these compounds bound to CD22Rg although, for some, with a significantly poorer affinity as indicated by a higher RIC. Compound **8** had a RIC 3-fold higher than its non-thio derivative (**6**), while **9** had a lower RIC than its non-thio derivative (**10**). However, this chemical modification did not produce dramatic changes in the apparent binding affinity of these compounds for CD22Rg.

Several C_6-methyl-Gal sialosides were similarly examined. This chemical modification limits the rotamer conformations possible with the Sia-Gal disaccharide. In aqueous solution, two rotamer orientations (tg and gt) are commonly found, formed by a 120° rotation around the C_5-C_6 bond in Gal. In one (gt), the two saccharide residues are bent back over themselves, and in the other (tg), the two residues are in an extended conformation (31). The (6*S*)- or (6*R*)-C_6-methyl group sterically limits this rotation and shifts the equilibrium in favor of one or the other of these two rotamers. These compounds have been useful in determining the orientation of the Sia-Gal disaccharide preferred by different sialidases, most of which show a

TABLE I
Summary of relative inhibitory concentrations (RIC) of sialylated and/or sulfated compounds as determined by ELISA competition assay

From the ELISA competition experiments presented in Figs. 3 and 4, the RIC (ratio of observed IC_{50} to that of α2–6sLac in the same assay) for each compound was calculated.

No.[a]	Compound[b]	RIC
1.	NeuAcα2–6Galβ1–4Glc	1.0
2.	NeuAcα2–6(6-thio)Gal diisopropylidene	1.0
3.	NeuAcα2–6(6-thio)Gal	2.3
4.	NeuAcα2–6Gal β-TMS	2.8
5.	NeuAcα2–3 Galβ1–4Glc	NI[c]
6.	NeuAcα2–6(6*R*)(6-Me)Gal β-TMS	4.3
7.	NeuAcα2–6(6*S*)(6-Me)(6-thio)Gal	10.0
8.	NeuAcα2–6(6*R*)(6-Me)(6-thio)Gal β-TMS	13
9.	NeuAcα2–6(6*S*)(6-Me)(6-thio)Gal β-TMS	13
10.	NeuAcα2–6(6*S*)(6-Me)Gal β-TMS	20
11.	NeuAcα2–6(6*R*)(6-Me)(6-thio) Gal diisopropylidene	50
12.	NeuAcα2–6Galβ1–3GlcNAc β-OBn	2.7
13.	NeuAcα2–6Galβ1–3GalNAc α-OBn	4.3
14.	6-O-SO_3Galβ1–3(NeuAcα2–6)GalNAc α-ONP	6.7
15.	Galβ1–3(NeuAcα2–6)GlcNAc β-OBn	13
16.	Galβ1–3(NeuAcα2–6)GalNAc α-OBn	30
17.	NeuAcα2–6GalNac α-ONP	0.33
18.	Galβ1–3(NeuAcα2–6)GlcNAc β-ONP	0.33
19.	6-*O*-SO_3Galβ1–3(NeuAcα2–6)GlcNAc β-ONP	0.33
20.	6-*O*-SO_3Galβ1–3GlcNAc β-ONP	NI[c]
21.	Galβ1–3(6-*O*-SO_3)GlcNAc β-OMe	NI[c]
22.	6-*O*-SO_3Galβ1–3GalNAc α-ONP	NI[c]
23.	Galβ1–3(6-*O*-SO_3)GalNAcα-*O*-allyl	NI[c]
24.	6-*O*-SO_3Galβ1–4Glc	NI[c]
25.	6-*O*-SO_3(Fucα1–2)Galβ1–4Glc	NI[c]
26.	NeuAcα2–6Galβ1–4GlcNAcβ1–4\ Gal-β-OR_1[d] NeuAcα2–6Galβ1–4GlcNAcβ1–2/	0.5
27.	NeuAcα2–6Galβ1–4GlcNAcβ1–6\ Gal-β-OR_1 NeuAcα2–6Galβ1–4GlcNAcβ1–3/	1.0
28.	NeuAcα2–6Galβ1–4GlcNAcβ1–6\ Gal-β-OR_1 NeuAcα2–6Galβ1–4GlcNAcβ1–4/	1.3
29.	NeuAcα2–6Galβ1–4GlcNAcβ1–6\ Gal-β-OR_1 NeuAcα2–6Galβ1–4GlcNAcβ1–2/	1.3
30.	Pooled AGP oligosaccharides[e]	1.3
31.	Sialylated fibrinogen glycopeptides[f]	2.7

[a] The numbering of the compounds corresponds to the numbering scheme used in Figs. 3 and 4.
[b] TMS, trimethylsilane; Bn, benzyl.
[c] No inhibition detected at highest concentration employed, as indicated in respective figure.
[d] R1 is -$(CH_2)_5COOCH_3$.
[e] Total PNGase F released oligosaccharides from AGP.
[f] A mixture of mono(α2–6)sialylated (25%) and bi(α2–6)sialylated (75%) glycopeptides.

marked preference for tg over the gt (31). For CD22Rg binding, the C_6-methyl derivatives all showed poorer RICs relative to non-methyl derivatives (Fig. 3*B* and Table I). However, the (6*S*)-C_6-methyl modification appeared to be more detrimental to sialoside binding (**6** *versus* **10**), indicating a preference for the tg rotamer. This preference is lost in the methyl-thio derivatives (**8**, **9**, and **11**), which are poorer inhibitors of CD22Rg-IgM binding.

A large number of different Sia α2–6-Hex(NAc) sialosides (with Hex(NAc) being GlcNAc, GalNAc, or Gal) are recognized by CD22Rg (Fig. 3, *C* and *D*, and Table I). A preference for GlcNAc over GalNAc is suggested by the different RICs of compounds **12** *versus* **13** and **15** *versus* **16**, although a difference in the linkage (α *versus* β) of the blocking groups may also explain the differences seen. CD22Rg binding was significantly influenced by the structure of the group attached to the Hex(NAc) residue. For example, the RIC of **18**, which has a ONP group attached to a GlcNAc residue, is 40-fold better than that of **15**, which contains a benzyl alcohol group instead. Addition-

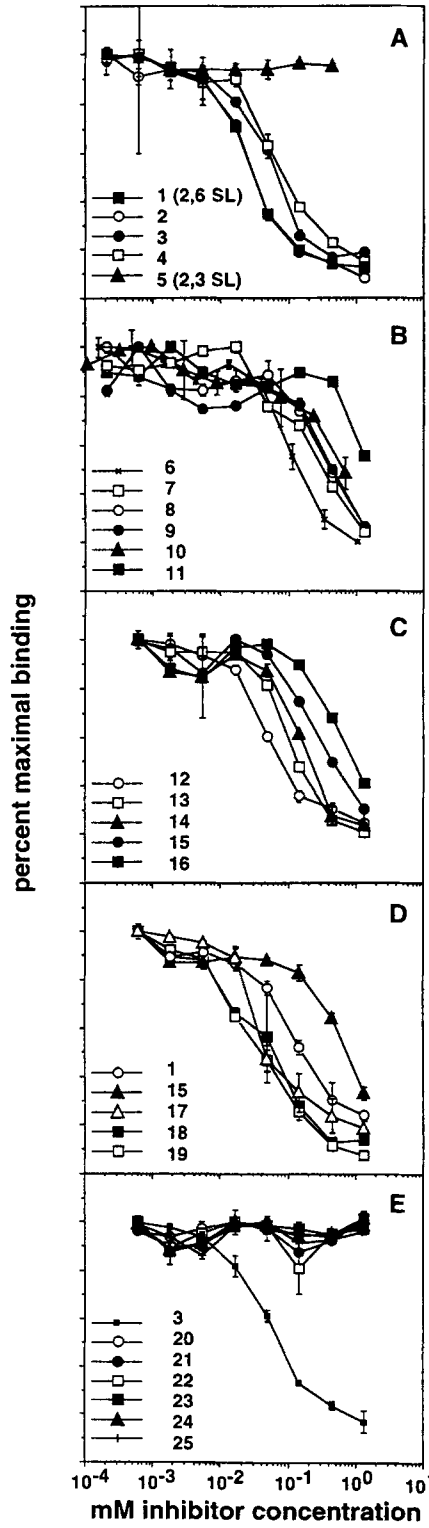

FIG. 3. **Structural parameters influencing the interaction of sialosides with CD22Rg.** The relative affinities of several different sialylated oligosaccharides for CD22Rg was inferred by determining their ability to inhibit the binding of CD22Rg to immobilized IgM in an ELISA assay. Binding was performed in the absence or presence of the indicated inhibitor at 4 °C for 12–15 h, and then bound CD22Rg determined as described under "Experimental Procedures." The different compounds tested are identified by number corresponding to the listing in Table I. The data presented are representative experiments, and each data point represents duplicates ± S.D. For each series of experiments performed on a given day, α2–6-sLac was included as a reference compound. The data presented in *Panels A, B,* and *C* are from one series of experiments, and the inhibition profile of α2–6-sLac is shown only in *Panel A* for simplicity.

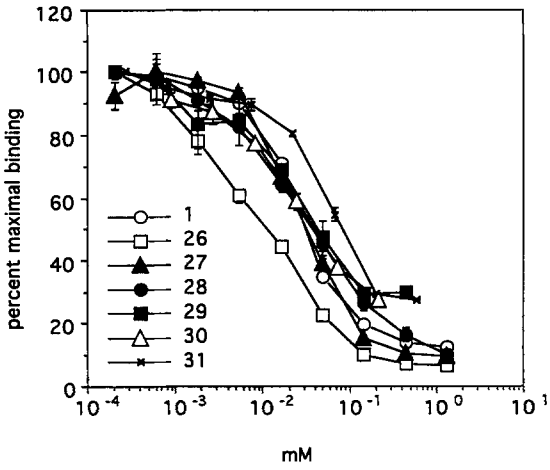

FIG. 4. **Inhibition of CD22Rg-IgM binding by bisialylated compounds.** Several synthetic or naturally occurring bisialylated compounds were examined in the ELISA assay. The different compounds tested are identified by number corresponding to the listing in Table I.

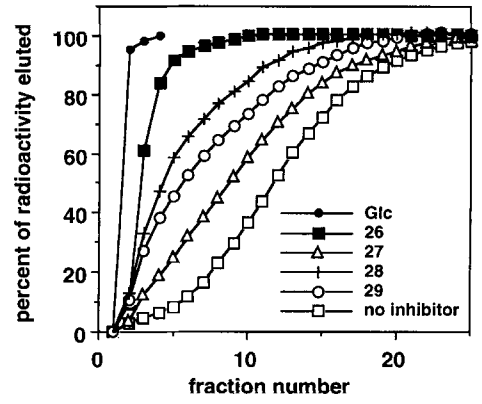

FIG. 5. **Demonstration of relative binding of bisialylated structures to CD22Rg.** Compounds **26–29** were screened for their ability to inhibit [^{3}H]FGP-CD22Rg binding in the column assay as described in Fig. 2, using a single concentration of 30 μM (based on Sia groups). The elution profiles are presented as a running sum. The elution profiles of [^{3}H]FGP in the absence of any inhibitor (*no inhibitor*) and of one typical profile of [^{14}C]Glc (*Glc*) are also shown.

ally, Glc is favored over trimethylsilane (compare **1** and **4**), and we previously demonstrated that Glc was favored over glucitol (37). Other pairs of compounds differing only in their reducing group were not available. Several structures based on the α2–6-sialylated Galβ1–3GalNAc/GlcNAc trisaccharide (**12** and **13**), which is not found in nature, also were reasonable inhibitors of CD22Rg-IgM binding. Moreover, significant modifications of the Hex(NAc) residue are permissible, including 3-*O*-galactosylation (compounds **15** and **16**) as well as capping O_1-O_4 with alkyl groups, as found in the diisopropylidene derivatives. Taken together, these results indicate that Siaα2–6Hex(NAc) sialosides are recognized by CD22Rg. These observations are significant as they indicate that a wide range of α2–6-sialylated structures, found on both *N*- and *O*-linked structures and glycolipids, may be potential ligands for CD22Rg.

Previously, we demonstrated that glycopeptides from bovine submaxillary mucin, a rich source of Siaα2–6GalNAcα-(peptide) residues, was not recognized with high affinity by CD22 even after de-*O*-acetylation of sialic acids (37). When this same bovine submaxillary mucin preparation was screened by the column assay as described in Fig. 2, a level of inhibition of [^{3}H]FGP binding corresponding to 30 μM α2–6-sLac was seen with 900 μM bovine submaxillary mucin (based on Sia concentration; data not shown), confirming our earlier result (37). Thus, the low RIC of compound **17** (Table I), which is comparable to the mucin structure must be explained either by a positive effect of the ONP aglycone, or by a negative effect of the polypeptide in the case of bovine submaxillary mucin.

Several modifications were without effect on sialoside binding. Sulfation did not affect the binding of sialylated compounds, and sulfate did not substitute for sialic acid (Fig. 3*E*). The sulfated derivative of **16** did exhibit a 4.5-fold improvement in its RIC (**16** *versus* **14**, Table I), yet these compounds also differ in their reducing terminus blocking group. As with **17**, **18**, and **19**, the ONP group improves the compound's RIC considerably.

Recognition of Bisialylated Structures by CD22Rg—Several bisialylated compounds were examined (Fig. 4; **26–31**, Table I). Included here were several synthetic bisialylated structures (**29–31**) as well as FGP glycopeptides and *N*-linked oligosaccharides released from AGP. The FGP preparation utilized here contained approximately 75% bisialylated structures (see "Experimental Procedures"). The AGP mixture utilized here contained a mixture of α2–6- and α2–3-linked residues in an approximate ratio of 1.2 to 1 (37) on a mixed population of bi-, tri-, and tetraantennary structures. Surprisingly, the RIC of all of these compounds, relative to α2–6-sLac, was approximately 1. The RIC for the FGP preparation, however, consistently was in the range of 2.5 to 3, whereas one of the synthetic bisialylated compounds (**26**) was 2-fold better. None of the bisialylated compounds exhibited RICs in the range of 0.03, as would be predicted from the equilibrium K_d values measured above. Moreover, the marked difference between α2–6-sLac and FGP seen in the CD22Rg-oligosaccharide column assay (Fig. 2) was not reflected in this ELISA assay. This apparent discrepancy probably reflects the intrinsic differences between these two assays, particularly for measuring binding events characterized by relatively fast on and off rates (unlike antibody-antigen binding, which is typically characterized by slow on and off rates). In the ELISA assay, multiple washing steps (lacking the inhibitor) are performed after the binding of the CD22Rg to the sialylated glycoprotein (which is done in the presence of the inhibitor). In contrast, in both the equilibrium dialysis experiments and in the column assay, the soluble oligosaccharide (as either a ligand or an inhibitor) is present throughout the binding process. Thus, these assays are fundamentally different, which may explain the apparently discrepant results in the inhibitory potency of the bisialylated compounds.

Given this limitation with the ELISA assay, compounds **26–29** were examined with the column retention assay, using each at a concentration of 30 μM. These results indicate measurable differences in the ability of these compounds to compete with the binding of the [^{3}H]FGP sample to CD22Rg, with **26** being the most potent inhibitor (Fig. 5). Although it would appear to be more potent than FGP at 30 μM, the FGP preparation contained a mixture of mono- and bisialylated structures. While these four sialosides are structurally very similar, they are all branching isomers and, consequently, the terminal α2–6-Sia residues will be oriented differently (29, 30). Molecular modeling predicts that the C_2-C_2 distance between the two Sia molecules is 17–19 Å for **26** and **29**, and 9–10 Å for **27** and **28** (29), thus, these measurements do not correlate with the different RICs seen for these four compounds (Table I). Other structural features, such as the relative orientation of the Siaα2–6Gal units, must be involved. Earlier we presented evidence indicating that CD22Rg was capable of discriminating between two different bi(Siaα2–6)-tetraantennary isomers, although we were not able to directly prove which antennae were sialylated (37). The observations with these four synthetic bisialylated compounds confirms our earlier hypothesis that

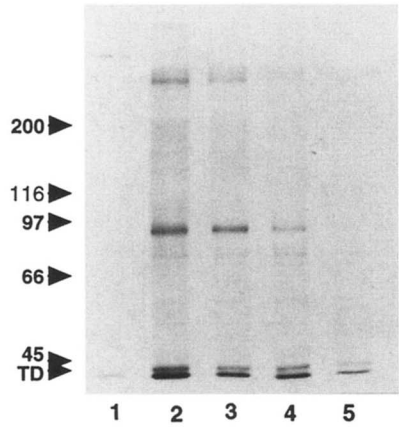

FIG. 6. **Inhibition of CD22Rg binding to Daudi cell glycoproteins by α2–6-sLac.** Equal aliquots of [^{35}S]Met-labeled Daudi cell lysate were precleared with protein A-Sepharose and then precipitated with CD22Rg and additional protein A-Sepharose in the presence of buffer alone (*lane 2*), or 30 μM (*lane 3*), 90 μM (*lane 4*), or 1 mM (*lane 5*) α2–6-sLac. Material nonspecifically adsorbed to an equal volume of protein A-Sepharose in the absence of CD22Rg is shown in *lane 1*. After boiling the beads with sample buffer, equal aliquots of the solubilized radioactivity were examined by SDS-PAGE analysis. Other aliquots were used to determine the amount loaded (cpm) of 800 (*lane 1*), 12,620 (*lane 2*), 6,860 (*lane 3*), 3,620 (*lane 4*), and 2,500 (*lane 5*); and to show that all of this radioactivity is trichloroacetic acid-precipitable (data not shown). *TD*, tracking dye.

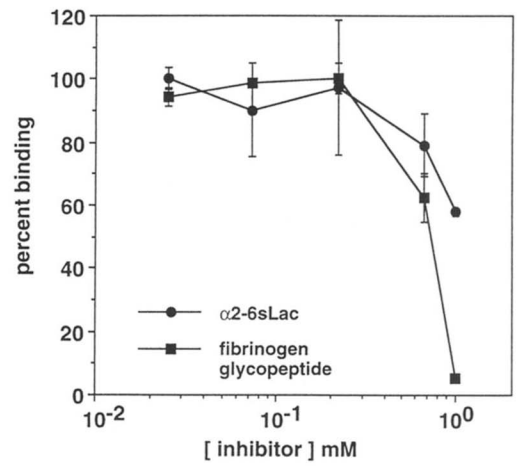

FIG. 7. **Inhibition of Daudi cell binding to CD22 expressing CHO cells by sialylated oligosaccharides.** Radiolabeled Daudi cells were allowed to bind to confluent cultures of CD22-CHO cells at 4 °C, and bound cells quantitated by scintillation counting. During the initial binding step, either α2–6-sLac (■) or FGP (mixture of mono- and bisialylated structures; ●) was included at the indicated concentrations. Each point represents the average of triplicate assays.

CD22Rg binding is influenced by the relative positioning of multiple Sia groups on a single oligosaccharide.

α2–6-sLac Inhibition of Precipitation of Daudi Glycoproteins by CD22Rg—Previous studies demonstrated that CD22Rg immunoprecipitates a spectrum of α2–6-sialylated glycoproteins from different T and B cell populations (8, 20, 21). An [^{35}S]Met-labeled lysate, prepared from Daudi cells, was precipitated with CD22Rg in the absence or presence of increasing amounts of α2–6-sLac. The overall pattern of precipitated proteins seen is similar to that published previously and is expected to include both glycoproteins and proteins associated with glycoproteins which bind to CD22Rg (8, 21). The results (Fig. 6) indicated that α2–6-sLac inhibited CD22Rg-glycoprotein binding in a range predicted by its K_d, with ~50% inhibition seen at 30 μM, further indicating that CD22Rg is functioning in these precipitation assays solely by recognition of α2–6-linked sialic acid residues. Of particular note, the binding of all precipitated proteins appeared to be equally sensitive to inhibition by α2–6-sLac, with the exception of the low molecular weight proteins which comigrate with proteins that nonspecifically adsorb to protein A-Sepharose (Fig. 6, *lanes 1* and *5*). It is known that many of the nonprecipitated Daudi cell glycoproteins also contain α2–6-linked sialic acid residues.[2] The segregation of different glycoproteins into either CD22Rg binding or nonbinding fractions must therefore be based on other factors, such as density of α2–6-sialic acid residues (which would control the ability of the chimera to form a precipitin reaction) or steric hindrance of α2–6-sialic acid residues by the protein structure (as was observed with transferrin (37)).

Inhibition of CD22-CHO Cell Binding to Daudi Cells—Given that all of these experiments were performed with the bivalent CD22Rg chimera, the question arises whether native CD22, expressed as a integral membrane protein, is capable of distinguishing between mono- and multiply sialylated oligosaccharide structures. No information is currently available on the quartenary structure of native CD22, and early studies indicated that it is not found as a disulfide-linked dimer (4). To probe this question, CHO cells were stably transfected with CD22β containing plasmid, to create a CD22-expressing subline. When grown as a monolayer, these cells are capable of binding Daudi cells, while the parental CHO cells do not (22). Binding can be partially inhibited by inclusion of α2–6-sLac or FGP. However, significantly different inhibition curves are seen with these two different compounds. With FGP, approximately 50% inhibition is observed at 300 μM, while less than 50% inhibition was seen at 1 mM α2–6-sLac (Fig. 7 and accompanying paper (22)). That the IC_{50} values for these compounds do not match that seen in the ELISA assay is not surprising, given the multivalent nature of cell-cell adhesion. However, the difference in inhibition seen with these two compounds is striking and reproducible. In additional experiments (not shown) 1 mM 2–6-sLac consistently gave only partial inhibition of CD22-CHO cell binding, and FGP at the same concentration always gave nearly complete inhibition. The extent of inhibition seen with 1 mM 2–6-sLac was somewhat variable, and may reflect variables such as the density of CD22 on the CHO cell surface (even though the cells were stably transfected, the levels of expression were not always consistent after extended culture). We therefore did not do an in depth study on 2–6-sLac inhibition and FGP inhibition *versus* CD22 density. Regardless, the ability of FGP to produce higher levels of inhibition at the same concentration (based on Sia content) suggests that CD22 molecules on the surface of the CHO-CD22 cell are in close enough proximity to allow a single FGP molecule to interact with more than one lectin binding site on two CD22 chains.

Cross-linking Studies of Cell-surface CD22—Given this result, the quartenary structure of cell-surface expressed CD22 was examined by cross-linking the metabolically labeled protein with a cleavable cross-linking reagent DTSSP. Low levels of DTSSP resulted in a partial reduction in intensity of the 140-kDa CD22β band concomitantly with the appearance of a high M_r band which barely entered a 6% SDS-polyacrylamide gel (Fig. 8). Cleavage of the cross-linker resulted in the loss of this high M_r band. No additional protein bands are seen following reduction, even on gels which are exposed for a considerably longer time, indicating that the high M_r band does not contain additional metabolically labeled (but low abundance or molecularly heterogenous) proteins. Moreover, the disappearance of the high molecular mass band (following reduction) is associated with an increase in the intensity of the 140-kDa

[2] L. D. Powell and A. Varki, unpublished data.

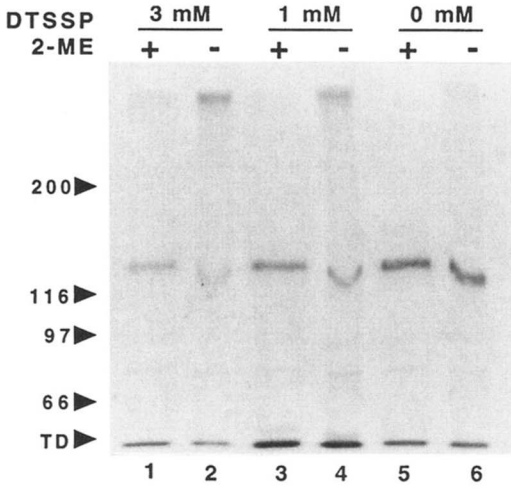

FIG. 8. **Cross-linking of CD22 on CD22 expressing CHO cells.** Cells metabolically labeled with [^{35}S]Met were cross-linked with the thio-cleavable agent, DTSSP, at the indicated concentration, and immunoprecipitated with mAb To15, directed against human CD22. After purification, one-half of each sample was reduced with 2-mercaptoethanol (*2-ME*), as indicated, and both reduced and nonreduced samples were analyzed on a 6% SDS-PAGE. The molecular weight standards are indicated on the *left*. *TD*, tracking dye.

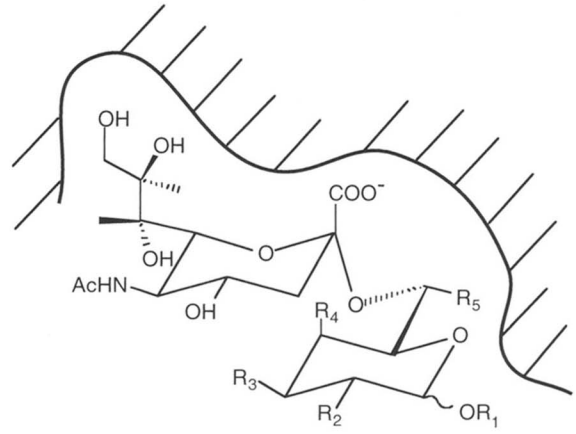

FIG. 9. **Proposed model of CD22-sialoside binding.** The disaccharide Siaα2–6Gal, in the tg rotamer conformation, is presented interacting with the binding pocket of CD22. This model is designed to incorporate the data presented in Table I, and under "Discussion." R_1: Gal, GlcNAc, GalNAc, trimethylsilane, benzyl, ONP, allyl, isopropylidene or H; R_2: isopropylidene, OH, or NAc; R_3: Gal, isopropylidene, or OH; R_4: isopropylidene or OH; and R_5: methyl or OH.

CD22β band, demonstrating that this high molecular mass band must contain at least some CD22 molecules. The bands migrating at the dye front adsorb to protein A-Sepharose in the absence of anti-CD22 and thus represent nonspecific contaminants. Thus, a portion of cell-surface CD22 must be present on the surface in a multimeric structure.

DISCUSSION

Previously, we established that the B cell sialic acid-binding protein, CD22, specifically recognized the trisaccharide Siaα2–6Galβ1–4GlcNAc as commonly found on *N*-linked oligosaccharides, but also on some *O*-linked oligosaccharides and glycolipids (21, 37). These studies were all accomplished with a column-binding assay, employing the bivalent immunoglobulin fusion construct CD22Rg bound to protein A-Sepharose, in which the elution of appropriately sialylated structures was significantly retarded beyond that of a nonbinding monosaccharide. Structures with more α2–6-Sia residues were separated from those with less Sia residues. This observation suggested the possibility of multivalent interaction between a multiply sialylated oligosaccharide and the bivalent CD22Rg construct. Alternatively, the better retention could be merely due to a statistical effect, *i.e.* increased probability of interactions with the column during the elution. The results described herein demonstrate that CD22Rg chimera has two binding sites for α2–6-sLac, each with a K_d of ~30 μM. Although equilibrium dialysis could not be performed on a bi(Siaα2–6)-biantennary oligosaccharide, additional studies indicated that this compound bound to CD22Rg with approximately 17-fold lower K_d. Additionally, a comparison of the inhibitory potency of several bisialylated oligosaccharides against α2–6-sLac in the column retention assay further supports the likelihood that simultaneous interaction is occurring. In these assays, the bisialylated compounds are clearly more potent inhibitors than α2–6-sLac when compared on an equimolar basis relative to α2–6-Sia groups, indicating that they have a higher affinity than α2–6-sLac alone. The work presented here and previously (21) has indicated that no other structural features in a multiantennary oligosaccharide are recognized by CD22Rg. Thus, the enhanced affinity of the bisialylated oligosaccharides is most likely due to the binding of CD22Rg to the two Siaα2–6Galβ1–4GlcNAc structures terminating the antennae. Extensive studies on antibody-hapten binding (reviewed in Ref. 26) would argue that this enhanced affinity is due to the simultaneous binding of the two Siaα2–6Galβ1–4GlcNAc moieties to CD22Rg. Unambiguous proof of this point, of course, would require direct equilibrium binding studies with mono- and bivalent forms of CD22 with mono- and bivalent sialylated oligosaccharides.

Even if a single multisialylated oligosaccharide does simultaneously interact with the two lectin binding sites of CD22, the latter is in fact an artificially created chimeric protein. It is more important to know if a similar phenomenon can occur with native full-length CD22β which is initially synthesized as a monomer. Indeed, two lines of investigation (inhibition of binding by oligosaccharides and cell surface cross-linking) suggest that the native molecule expressed on the surface of CHO cells, associates to form noncovalent oligomers. This multimeric association offers a mechanism of producing a higher apparent binding affinity than would be observed with single chain CD22.

Collectively, the results obtained with the different monosialylated compounds examined in Table I indicate that the minimum structure required for CD22Rg binding is Siaα2–6-Hex(NAc), where Hex(NAc) is Gal, GalNAc, or GlcNAc. An examination of the different RICs of the compounds listed in Table I, together with our earlier studies offers considerable insight into the regions of the sialoside which are recognized by the protein. Fig. 9 shows Neu5Acα2–6Galβ1-R in the tg rotamer (the gt rotamer is formed by a 120 °C rotation around the Gal C_5-C_6 bond), and we propose a model for CD22-sialoside binding based on these data and earlier studies (13, 21, 39). The C_7-C_8-C_9 side chain of Sia is essential for binding, as either its removal or its 9-*O*-acetylation abolishes binding (13, 20, 21). The N_5 substituent on Sia (glycolyl *versus* acetyl) may be in close proximity to the binding site, as the murine form of CD22 shows a partial preference for Neu5Gc over Neu5Ac (a preference not seen with human CD22) (11). The Gal O_5-C_6 face of this disaccharide must also be involved in CD22 binding as these positions are the key structural features which distinguish α2–6-sLac from α2–3-sLac. The generally unfavorable effect of C_6 methylation of Gal likewise indicates that this region of the disaccharide faces the binding site. In contrast, the other hydroxyl groups of the Gal residue are not involved in CD22 binding, as (*a*) α2–6-sialylated Gal, GalNAc, and GlcNAc are all recognized; (*b*) capping some or all of the hydroxyl

groups with alkyl groups (as in the case of the di-*O*-isopropylidene derivative) or with an additional Gal residue was without effect on binding; (*c*) the configuration at Gal C_4 is not significant (as both α2–6-sialylated GalNAc and GlcNAc are recognized). The group at the reducing terminus of Gal (R_1 in Fig. 9) must also face against the protein (as opposed to being oriented out into the solvent) as different blocking groups at this position (trimethylsilane, benzyl, ONP, H, Glc, Glc-OH, or peptide) markedly influence binding. Thus, we would predict that the CD22 binding site would be an area sufficiently large to accommodate these multiple points of contact.

The binding specificity of CD22 is somewhat comparable to that of the lectin SNA. As studied by precipitation assays, this lectin is specific for the sequence Siaα2–6Gal/GalNAc, with a K_d (by equilibrium dialysis) of 2.5 μM (25, 40). As with CD22, the C_7-C_8-C_9 side chain of Sia is required for binding (40). Unlike CD22, however, SNA recognizes additional structural determinants in an oligosaccharide structure, as evidenced by the 100-fold greater inhibitory potency of Siaα2–6Galβ1–4GlcNAcβ1–3Galβ1–4Glc over α2–6-sLac (40). Moreover, lactose at concentrations of 0.1 M are capable of inhibiting SNA-oligosaccharide binding (25, 40), an effect which is not found with CD22Rg (37). Mucins containing the Siaα2–6GalNAc sequence bind well to SNA (judged by a precipitin assay) (40), while preparations of such mucins bind very poorly to CD22 (37). While 9-*O*-acetylated α2–6-Sia groups are not recognized by CD22, it is not known if SNA binding can be affected by this substitutions. 6-Thio derivatives are not recognized by SNA, nor does it show preferential binding to any of the synthetic disialosides examined here (**26–29**) (29, 30).

The CD22Rg chimera was constructed to be bivalent by inclusion of the hinge region of IgG. The ability of a bi(Siaα2–6)-biantennary oligosaccharide to simultaneously interact with both binding sites is indicated by the higher levels of inhibition of the bisialylated compounds over α2–6-sLac, both in the cell binding assay and the column assay. The different levels of inhibition achieved by synthetic bisialylated compounds **26–29** indicate that the construct shows a preference for certain branching orientations. The ability of multiantennary oligosaccharides to simultaneously interact with multiple binding sites on multisubunit lectins has been demonstrated with several lectins (29, 41–44). One well studied example is the hepatic Gal/GalNAc lectin. This protein is a trimer, with each monomer containing two Gal/GalNAc binding sites. An oligosaccharide with a single Gal residue on its nonreducing terminus binds with a K_d of 1 mM, and branched structures containing two and three terminal Gal residues bind with affinities approximately 10^3 and 10^6 tighter, respectively (41, 43, 45). Likewise, the affinity of the cation-independent Man-6-phosphate receptor, which contains two binding sites, for ligands containing two Man-6-P groups is 300-fold higher than for ligands containing just one (44). From basic thermodynamic principles, the apparent K_d for dimeric receptor-ligand binding should be the product of each individual binding interaction; the extent that this theoretical limit is not met is reflective of strain or steric factors which limit the simultaneous independent interaction of the two receptor-ligand pairs (26). The differences in apparent binding affinity of the different bisialylated compounds (**26-29**; Table I) is indicative that the two Sia binding sites on CD22Rg are not optimally oriented for all bisialylated structures, *i.e.* that different levels of intramolecular strain are induced in these compounds when bound to CD22Rg.

The inability of the ELISA assay to detect the bivalent nature of oligosaccharide recognition is surprising and without obvious explanation. However, the ELISA capture assay, involving a primary binding and then a secondary reagent, with multiple washing steps in between, is very different from a solution phase equilibrium or column assay. This discrepancy indicates that ELISA capture assays may not always be the best assay for describing interactions which may potentially be multivalent.

The binding affinity for a monovalent ligand seen here, ~30 μM, is in line with that observed for other lectin-oligosaccharide interactions (45). For a single receptor-ligand interaction, this affinity is comparatively low and would suggest that in nature, CD22's function as an adhesion molecule is dependent upon multiple interactions. Conversely, it is possible that higher affinity interactions will be found with naturally occurring ligands. The CD22-containing oligomers we have reported here may be part of a mechanism to create a receptor structure capable of distinguishing between different α2–6-sialyloligosaccharides. Such a mechanism(s) could be very important in the role(s) CD22 plays in cell-cell adhesion and signaling.

The cross-linking studies presented here indicate that native CD22 may also utilize multivalency to achieve functional interactions. No dimers were seen in these studies, indicating that at least a portion of cell-surface CD22 exists in a multimeric state. Also, no association was seen with any other metabolically-labeled proteins, implying that these complexes are homomultimers. In support of this, the intensity of the CD22 monomer band decreased in the presence of the cross-linker to an extent qualitatively consistent with the appearance of the multimer bands. Furthermore, the anti-CD22 antibody adsorbed less than 0.2% of the total macromolecular [^{35}S]Met material, and in the presence of the cross-linker, the total amount of counts/min adsorbed to To15/protein A-Sepharose was ~75% of that in its absence. If CD22 were being cross-linked to a heterogeneous array of different proteins (and thus not visible as a discrete band after reduction) then the amount of counts/min would be expected to increase in the presence of the cross-linking agent. Of course, we cannot rule out the presence of non-labeled proteins in these multimers (either long-lived or poor in Met/Cys residues). Regardless, since CHO cells (a fibroblastic cell line) are capable of supporting the formation of these multimers, we can be certain that no B lymphocyte-specific proteins are required. It is possible that the CD22 molecules self-associate in the membrane following biosynthesis. In this regard, CD22 might be similar to the cation-dependent Man-6-P receptor, which although it has a stoichiometry of 1:1 for the cognate oligosaccharide (46), is able to generate high-affinity binding via the reversible formation of dimers and multimers (47–49).

Acknowledgments—We acknowledge the technical assistance of Jeannette Moyer and Jennifer Callow, and thank Graham Long for his careful review of the manuscript.

REFERENCES

1. Dorken, B., Moldenhauer, G., Pezzutto, A., Schwartz, R., Feller, A., Kiesel, S., and Nadler, L. M. (1986) *J. Immunol.* **136,** 4470–4479
2. Law, C.-L., Sidorenko, S. P., and Clark, E. A. (1994) *Immunol. Today* **15,** 442–449
3. Pezzutto, A., Dorken, B., Moldenhauer, G., and Clark, E. A. (1987) *J. Immunol.* **138,** 98–103
4. Boue, D. R., and Lebien, T. W. (1988) *J. Immunol.* **140,** 192–199
5. Boue, D. R., and Lebien, T. W. (1988) *Blood* **71,** 1480–1486
6. Stamenkovic, I., and Seed, B. (1990) *Nature* **345,** 74–77
7. Wilson, G. L., Fox, C. H., Fauci, A. S., and Kehrl, J. H. (1991) *J. Exp. Med.* **173,** 137–146
8. Stamenkovic, I., Sgroi, D., Aruffo, A., Sy, M. S., and Anderson, T. (1991) *Cell* **66,** 1133–1144
9. Torres, R. M., Law, C. L., Santos-Argumedo, L., Kirkham, P. A., Grabstein, K., Parkhouse, R. M., and Clark, E. A. (1992) *J. Immunol.* **149,** 2641–2649
10. Engel, P., Nojima, Y., Rothstein, D., Zhou, L. J., Wilson, G. L., Kehrl, J. H., and Tedder, T. F. (1993) *J. Immunol.* **150,** 4719–4732
11. Kelm, S., Schauer, R., Manuguerra, J-C., Gross, H-J., and Crocker, P. R. (1994) *Glycoconj. J.* **11,** 120–126
12. Aruffo, A., Kanner, S. B., Sgroi, D., Ledbetter, J. A., and Stamenkovic, I. (1992) *Proc. Natl. Acad. Sci. U. S. A.* **89,** 10242–10246
13. Sjoberg, E. R., Powell, L. D., Klein, A., and Varki, A. (1994) *J. Cell Biol.* **126,**

549–562
14. Paulson, J. C., Rearick, J. I., and Hill, R. L. (1977) *J. Biol. Chem.* **252,** 2363–2371
15. Weinstein, J., de Souza-e-Silva, U., and Paulson, J. C. (1982) *J. Biol. Chem.* **257,** 13835–13844
16. Pezzutto, A., Rabinovitch, P. S., Dorken, B., Moldenhauer, G., and Clark, E. A. (1988) *J. Immunol.* **140,** 1791–1795
17. Schultz, P. G., Campbell, M.-A., Fischer, W. H., and Sefton, B. M. (1992) *Science* **258,** 1001–1004
18. Peaker, C. J., and Neuberger, M. S. (1993) *Eur. J. Immunol.* **23,** 1358–1363
19. Leprince, C., Draves, K. E., Geahlen, R. L., Ledbetter, J. A., and Clark, E. A. (1993) *Proc. Natl. Acad. Sci. U. S. A.* **90,** 3236–3240
20. Sgroi, D., Varki, A., Braesch-Andersen, S., and Stamenkovic, I. (1993) *J. Biol. Chem.* **268,** 7011–7018
21. Powell, L. D., Sgroi, D., Sjoberg, E. R., Stamenkovic, I., and Varki, A. (1993) *J. Biol. Chem.* **268,** 7019–7027
22. Hanasaki, K., Varki, A., and Powell, L. D. (1995) *J. Biol. Chem.* **270,** 7533–7542
23. Hanasaki, K., Powell, L. D., and Varki, A. (1995) *J. Biol. Chem.* **270,** 7543–7550
24. Lee, E. U., Roth, J., and Paulson, J. C. (1989) *J. Biol. Chem.* **264,** 13848–13855
25. Shibuya, N., Tazaki, K., Song, Z., Tarr, G. E., Goldstein, I. J., and Peumans, W. J. (1989) *J. Biochem. (Tokyo)* **106,** 1098–1103
26. Berzofsky, J. A., Epstein, S. L., and Berkower, I. J. (1989) in *Fundamental Immunology* (Paul, W. E., ed) pp. 315–353, Raven Press, New York
27. Mopper, K., and Gindler, E. M. (1973) *Anal. Biochem.* **56,** 440–442
28. Wang, W. C., and Cummings, R. D. (1988) *J. Biol. Chem.* **263,** 4576–4585
29. Sabesan, S., Duus, J. O., Neira, S., Domaille, P., Kelm, S., Paulson, J. C., and Bock, K. (1992) *J. Am. Chem. Soc.* **114,** 8363–8374
30. Gupta, D., Sabesan, S., and Brewer, C. F. (1993) *Eur. J. Biochem.* **216,** 789–797
31. Sabesan, S., Neira, S., Davidson, F., Duus, J. O., and Bock, K. (1994) *J. Am. Chem. Soc.* **116,** 1616–1634
32. Chandrasekaran, E. V., Jain, R. K., Larsen, R. D., Wlasichuk, K., and Matta, K. L. (1995) *Biochemistry,* in press
33. Jain, R. K. and Matta, K. L. (1994) *XVIIth International Carbohydrate Symposium, July 17–22, 1994, Ottawa, Ontario,* **C2.6,** 443, National Research Council of Canada, Ottawa, Ontario, Canada
34. Jain, R. K., Piskorz, C. F., and Matta, K. L. (1995) *Carbohydrate Res.*, in press
35. Vig, R., Jain, R. K., and Matta, K. L. (1994) *Carbohydrate Res.*, in press
36. Shukla, A. K., and Schauer, R. (1982) *Hoppe-Seyler's Z. Physiol. Chem.* **363,** 255–262
37. Powell, L. D., and Varki, A. (1994) *J. Biol. Chem.* **269,** 10628–10636
38. Debeire, P., Montreuil, J., Moczar, E., van Halbeek, H., and Vliegenthart, J. F. (1985) *Eur. J. Biochem.* **151,** 607–611
39. Blinkovsky, A. M., and Dordick, J. S. (1993) *Tetrahedron: Asymmetry* **4,** 1221–1228
40. Shibuya, N., Goldstein, I. J., Broekaert, W. F., Nsimba-Lubaki, M., Peeters, B., and Peumans, W. J. (1987) *J. Biol. Chem.* **262,** 1596–1601
41. Baenziger, J. U., and Maynard, Y. (1980) *J. Biol. Chem.* **255,** 4607–4613
42. Baenziger, J. U., and Fiete, D. (1979) *J. Biol. Chem.* **254,** 9795–9799
43. Lee, Y. C., Townsend, R. R., Hardy, M. R., Lonngren, J., Arnarp, J., Haraldsson, M., and Lonn, H. (1983) *J. Biol. Chem.* **258,** 199–202
44. Tong, P. Y., Gregory, W., and Kornfeld, S. (1989) *J. Biol. Chem.* **264,** 7962–7969
45. Lee, Y. C., and Lee, R. T. (1994) *Neoglycoconjugates: Preparation and Applications,* Academic Press, San Diego, CA
46. Tong, P. Y., and Kornfeld, S. (1989) *J. Biol. Chem.* **264,** 7970–7975
47. Dahms, N. M., and Kornfeld, S. (1989) *J. Biol. Chem.* **264,** 11458–11467
48. Hille, A., Waheed, A., and von Figura, K. (1989) *J. Biol. Chem.* **264,** 13460–13467
49. Waheed, A., Hille, A., Junghans, U., and von Figura, K. (1990) *Biochemistry* **29,** 2449–2455